Fall 2022

EFFECT OF PRE-EXISTING FAULT ORIENTATION ON STRAIN LOCALIZATION IN A FOLIATED GRANITIC GNEISS

Geoffrey Hilliard
gh55@uakron.edu

EFFECT OF PRE-EXISTING FAULT ORIENTATION ON STRAIN LOCALIZATION IN A FOLIATED GRANITIC GNEISS

Geoffrey T. Hilliard

Advisor: Dr. Caleb Holyoke

Department of Geosciences

The University of Akron

December 2nd, 2022

Abstract

The effect of fault orientation relative to the applied stress on reactivation of pre-existing brittle faults instead of forming new faults is well-explained by Mohr-Coulomb theory. However, Mohr-Coulomb theory does not explain the effect of orientation on reactivation of faults with a ductile rheology and no work has been performed to assess the effect of orientation of a pre-existing ductile fault on fault strength. In order to determine how rock strength and localization of strain into a ductile fault is affected when the orientation of the pre-existing fault (artificial fault) is changed, experiments were performed on pre-faulted cores of a fine grained (d = 150 μm) granitic gneiss at a pressure of 1500 MPa, temperature of 750°C, and axial strain rate of 6.8×10^{-7} s^{-1}. The foliation of the gneiss was oriented 45° to the vertical compression direction and the artificial faults were cross cutting the foliation at 45° or 60° to the compression direction. Strain localized into the pre-fault oriented at 45° to the foliation. However, strain was accommodated by the host rock and a new shear zone along the foliation plane that crosscuts the artificial fault oriented at 60° to the compression direction. These results indicate that, like in brittle faults, the range of possible orientations for ductile fault reactivation is limited, and that reactivation of preexisting faults may not always occur in orogenies with multiple deformation events.

Introduction

Due to higher temperatures and pressures, rock deforms plastically throughout the Earth's mid to lower crust and the rheology of the lower crust at plate boundaries is controlled by deformation in ductile shear zones. These ductile shear zones are connected to brittle faults (brittle shear zones) in Earth's upper crust which deforms at lower temperatures and pressures than the lower crust. Modeling of the earthquake cycle has demonstrated that the intensity and quantity of aftershocks may be intimately related to the rheology of shear zones in the lower crust (Burgmann and Dresen, 2008). In addition, during extensive orogenic events that involve multiple deformation events, inactive faults can be reactivated instead of new faults being formed (Sibson, 1985). The effect of the fault orientation to the applied stress on reactivation of pre-existing brittle faults instead of forming new faults is well explained by Mohr-Coulomb theory (Sibson, 1985). However, Mohr-Coulomb theory does not explain the effect of fault orientation on reactivation of brittle faults at high temperatures and pressures that activate crystal plastic mechanisms forming ductile shear zones and no work has been performed to assess the effect of orientation on the strength of these ductile shear zones.

Previous experiments and field studies have determined that fine-grained material produced by brittle processes (gouge) can cause subsequent strain localization at high temperatures due to deformation by grain size sensitive mechanisms (Tullis and Yund, 1991; Guermani and Pennacchioni, 1998; Mancktelow and Pennacchioni, 2005). Fine-grained zones in feldspathic rock deform by recrystallization-accommodated dislocation creep or diffusion creep and are weaker than surrounding coarse grained feldspathic rock (Tullis and Yund, 1991). Tullis et al. (1990) observed that in a pre-faulted quartzite, strain was accommodated homogeneously throughout the quartzite. However, in pre-faulted samples of feldspathic rocks (Enfield aplite and fine-grained Hale/Tanco albite), strain localized in the pre-fault. Kullburg (2021) performed experiments on a foliated, feldspathic gneiss with a pre-fault oriented at approximately 25° to the compression direction but changed the orientation of foliation relative

to the fault and the compression direction. Kullberg (2021) observed that strain always localized in the pre-existing fine-grained fault, regardless of the foliation orientation, and that rock strength was greatly dependent on localization of deformation within the fault. He attributed this localization to deformation by grain-size sensitive mechanisms in the fine-grained fault zones. However, all these studies have faults in a similar, easy-slip orientation (25°) to the compression direction and have not determined how the orientation of ductile faults relative to the compression direction affects strain localization.

Methods

In order to determine the effect of orientation on reactivation of preexisting faults in a foliated rock, I performed experiments on cores of Gneiss Minuti in a Griggs-type piston rock deformation apparatus at a temperature (T) of 700°C, pressure (P_c) of 1500 MPa, and strain rate ($\dot{\varepsilon}$) of 6.8×10^{-7} s^{-1}. Deformation of a similar layer of Gneiss Minuti without a preexisting fault at these conditions by Holyoke and Tullis (2006) caused deformation by crystal plastic mechanisms similar to those operating in the middle continental crust.

The Gneiss Minuti is a fine-grained (~100 μm), compositionally-layered granitic gneiss originating from the Swiss Alps in Northern Italy (Zurbriggen et al., 1998; Fig. 1). I used a relatively homogeneous layer that contains plagioclase (53 vol%), quartz (29 vol%), potassium feldspar (10 vol%), biotite (7 vol%) and accessory garnet/Fe- Ti oxides (1 vol%), which was also used by Kullberg (2021). Biotite, quartz, and k-feldspar are isolated within a plagioclase framework (Fig. 1). Foliation in this layer is defined by aligned biotite grains and elongation of other phases.

I use the terms fault, ductile shear zone, pre-fault and artificial faults to describe different faults in this thesis. A fault is a localized zone of deformation that deforms primarily by brittle mechanisms. A ductile shear zone is a localized zone of deformation that deforms primarily by crystal plastic mechanisms. A pre-fault is a fault formed by brittle mechanisms at low

temperatures but is then deformed by crystal plastic mechanisms at higher temperatures. An artificial fault is a zone of mixed-grain size material that is installed in a cylinder by cutting a slice across the rock cylinder and placing mixed grain-size powders in between the cylinder halves. Pre-faults have been used successfully to explore formation of ductile shear zones by reactivation of brittle faults by Tullis et al. (1990) and Kullberg (2021), but the orientation of these faults is limited to 25-30° relative to the compression direction. I have made artificial faults in the rocks I deformed in order to change the orientation of the pre-existing zone of angular, mixed grain-size material, similar to that formed by a brittle fault, relative to the compression direction.

The Gneiss Minuti cylinders (~5 x 10 mm) were all cored from the rock with the foliation orientation at 45° to the compression direction (Fig. 2). Orienting the foliation at 45° to the length of the cylinders maximized shear stress along the foliation plane. Cuts to create artificial faults in the cores were made at 45° or 60° to the compression direction, crosscutting the foliation, but with the same strike as the foliation (Fig. 2). The preexisting faults in these experiments are artificial due to them being cut before experimentation, as opposed to forming during pressurization as in Kullberg (2021). Scraps of the same layer of Gneiss Minuti were ground into a fine but mixed grain-size powder (d = 1-100 μm) and placed inside the saw-cut with about a 0.5 mm thickness to simulate a fault gouge. The mineral grains within the powder became dense as they annealed during pressurization and sat hydrostatically at high temperature before deformation. Cutting the artificial faults in different orientations relative to the foliation tested whether localizing strain in the fault is easier than forming a new shear zone along the pre-existing foliation in its weakest orientation. If foliation strength controlled the strength of the rock, deformation would have occurred along the foliation plane. If the fault strength controlled the strength of the rock, deformation would have occurred along the fault.

Experiments were performed in a Griggs-type piston cylinder apparatus (Fig. 3; Griggs apparatus). Initially, two experiments were performed using Ag jackets about the outer edge of

the cylinder, but both experiments deformed prior to reaching final P/T conditions due to compaction of the porous powders during pressurization (Appendix 1). The results of these experiments are not considered here because the starting conditions of the artificial fault and host rock when deformation began are unknown. In order to prevent this deformation, I jacketed all subsequent experiments using a thick Ni jacket, which is strong at low temperatures (T = 25-300°C) in early pressurization and prevents deformation of the samples during pressurization. Unfortunately, Ni is also relatively strong at T = 750°C, so I performed an experiment using a Cu cylinder inside a thick Ni jacket. The strength of Cu at T = 750°C is <1 MPa (Frost and Ashby, 1982) and less than is measurable in the Griggs apparatus using a solid salt assembly, so the strength measured in the experiment is controlled by the Ni jacket. The final strength of the Ni-jacketed Cu was ~300 MPa (Fig. 4) and the stress-strain relationship before reaching this value was fit using third order linear regression. These data were used to correct the mechanical data of Gneiss Minuti experiments to the strength of the thick Ni jackets. The mechanical data from these experiments was also corrected using the methods described in Holyoke and Kronenberg (2010).

Gneiss Minuti cylinders were put in a solid salt assembly, within a NaCl confining medium with a graphite furnace to apply heat (Fig. 3). The cores were taken to pressure/temperature conditions slowly over about a 5-hour period to avoid deforming the core before load was applied. The temperature was monitored by a K-type thermocouple near the center of the cylinder. The load piston was advanced at a rate of 28 μm/hr and deformed the cylinder. After reaching the desired amount of strain, the experiments were quenched and depressurized to room conditions.

Cylinders were cut parallel to the loading direction and perpendicular to the fault/foliation. These cut surfaces were ground and polished prior to imaging with a scanning electron microscope (SEM) using backscattered electrons (BSE). BSE-SEM images of the cylinders were taken with the compression direction vertical.

Results

Three experiments were conducted on artificially faulted cores of Gneiss Minuti at T = 750°C, P_c = 1500 MPa, and $\dot{\varepsilon}$ = 6.8x10^{-7} s^{-1} to determine how fault orientation affects strain localization (Table 1).

One low strain (ε = 8%) experiment was performed on a cylinder with an artificial fault at 45° to the compression direction. The strength increased until the experiment was stopped at a differential stress of 600 MPa (Fig. 5). Strain was localized within the artificial fault and no evidence of deformation was observed in the host rock (Fig. 6).

One high strain (ε = 40%) experiment was performed on a cylinder with an artificial fault at 45° to the compression direction. Differential stress increased until reaching the peak stress (740 MPa, ε = 9%), before strain weakening to 380 MPa (ε = 40%; Fig. 5). Strain localized primarily in the artificial fault and no new shear zones formed along the foliation (Fig. 7). Within the artificial fault all phases, especially biotite which forms mica fish, are oriented parallel to the angle of the artificial fault (Fig. 8). However, outside of the artificial fault the foliation is locally rotated towards the shear zone (Fig. 9).

One high strain (ε = 34%) experiment was performed on a cylinder with an artificial fault at 60° to the compression direction. Differential stress increased until reaching the peak stress (670 MPa, ε = 14%) prior to strain weakening to 560 MPa (Fig. 5). A new shear zone formed sub-parallel to the foliation plane. This shear zone crosscuts the artificial fault (Fig. 10). Smaller offsets of material within the artificial fault parallel to the foliation are present in other sections of the artificial fault (Fig. 11). Recrystallized grains within the artificial fault are oriented parallel to the artificial fault, likely due to compression during pressurization and annealing. The foliation in the host rock is significantly rotated within 1.5 mm of the shear zone and slightly rotated elsewhere in the host rock (Fig. 12).

Discussion

I performed deformation experiments on cores of a fine-grained, foliated gneiss with artificial faults in two orientations to test how fault orientation affects fault reactivation due to crystal plastic deformation mechanisms under high pressure and temperature conditions. The low strain experiment performed on a core with an artificial fault at 45^{o} to the compression direction reached a peak stress of 600 MPa at 8% strain when the experiment was stopped. The host rock is undeformed, and strain is localized within the artificial fault. Both high strain experiments had high peak strengths (45°: 740 MPa at 9% strain; 60°: 670 MPa at 14% strain) prior to strain weakening until the end of the experiments (Fig. 5). The experiment with an artificial fault at 45° to the compression direction weakened by 360 MPa (49% of peak stress; Fig. 5) after reaching peak stress. The host rock is relatively undeformed and grains in the artificial fault are highly sheared (Fig. 7). Whereas, the experiment with an artificial fault at 60° to the compression direction only weakened by 110 MPa (16% of peak stress; Fig. 5) after reaching peak stress. The foliation in the host rock is pervasively rotated towards the shear zone, a new shear zone sub-parallel to the foliation crosscuts the artificial fault and the grains in the artificial fault are flattened with little evidence of shearing (Fig. 10). These results indicate that strain was primarily localized within the artificial faults in the samples with artificial faults at 45^{o} to the compression direction and this localization enabled greater strain weakening than the sample with a pre-fault which had more homogeneous strain in the host rock.

Holyoke and Tullis (2006) performed general shear geometry experiments on a similar layer of Gneiss Minuti (58% quartz, 28% plagioclase, 13% biotite) at a slightly faster shear strain rate ($2x10^{-6}\,s^{-1}$), and similar temperature (745^{o}C) and pressure (1.5 GPa) as my experiments. The foliation of these experiments was oriented at 45° to the compression direction, but the shear slice did not contain a pre-fault. The differential stresses were somewhat higher in their experiments (820-930 MPa) than in my experiments (670-740 MPa), consistent with

deformation at a greater strain rate than in my experiments. They observed that at low shear strains similar to my axial compression experiments, strain was localized in a single strand of interconnected biotite grains, similar to the small shear zone that formed in the core deformed with a pre-fault at 60°. In addition, they performed transmission electron microscopy analyses on their samples and observed that quartz deformed by recrystallization-accommodated dislocation creep, plagioclase deformed by semi-brittle flow which formed fine recrystallized grains, and biotite deformed by kinking and shearing along (001). The SEM-scale microstructures observed in their samples are similar to those present in my samples, indicating that the same deformation mechanisms are operating in the host rock portions of my experiments.

Kullberg (2021) performed experiments on the same layer of Gneiss Minuti that I used in my experiments and at similar conditions as my experiments (T = 700°C, P_c = 1.5 GPa, and $\dot{\varepsilon}$ = $2x10^{-7}$ s^{-1}). His cores had a pre-fault in a weak orientation (25° to the compression direction). He observed that comminution of the material in the pre-fault produced a starting grain size range similar to those observed in my pre-faults. This grain size reduction resulted in strain weakening by grain-size sensitive deformation mechanisms (diffusion creep/grain boundary sliding). His results indicated that grain boundary sliding is important to the initiation of ductile shear zones and localization of strain. Therefore, it is likely that in my experiments with an artificial fault at 45°, deformation within the fine-grained shear zone was likely driven by grain boundary sliding, due to the reduced grain size within the artificial fault.

Tullis et al. (1990) deformed cores of polycrystalline Hale/Tanco albite, Enfield aplite (1/3 quartz and 2/3 feldspar) and quartzite with pre-faults oriented at 25-30° to the compression direction. Similar to Kullberg (2021), these faults were created at low temperature and pressure (T = 300°C and P_c = 0.5 GPa) and these pre-faulted cores were subsequently taken to high temperature and pressure (T = 900°C and P_c = 1.5 GPa) to encourage deformation by crystal plastic deformation mechanisms. They observed that in pre-faulted feldspathic rock (Enfield

aplite and Hale/Tanco albite), strain localized in a ductile shear zone. They attributed this localization to deformation by grain-size sensitive deformation mechanisms including diffusion creep or recrystallization accommodated dislocation creep. In contrast, strain did not localize in a ductile shear zone in pre-faulted quartzite, but instead the sample deformed homogeneously. They attributed this homogeneous strain to deformation of quartz by a grain-size insensitive deformation mechanism, climb-accommodated dislocation creep. In both of my cores with an artificial fault oriented at 45° to the compression direction, strain localized within the artificial fault, consistent with the feldspathic rocks deformed by Tullis, et al. (1990). However, despite having a similarly fine-grained starting material in the artificial fault oriented at 60° to the compression direction, the host rock accommodated most of the strain in this sample. These results indicate that there is a limited range of orientations where a preexisting fault within a feldspathic rock can be reactivated and not all preexisting faults will be reactivated during complex orogenies with multiple deformation events.

Conclusion

I performed experiments on cores of Gneiss Minuti with artificial faults at two orientations relative to the compression direction (45^o and 60^o) and foliation in a weak orientation relative to the compression direction (45^o) at T = 750°C, P_c = 1500 MPa, and $\dot{\varepsilon}$ = 6.8x10^{-7} s^{-1}. Depending on the orientation of the artificial fault, strain either localized in the artificial fault (45^o) or the surrounding host rock (60^o). These results indicate that in nature it is likely that:

1. A preexisting fault in a weak orientation (45°) to the compression direction will be reactivated as a ductile shear zone due to the fine-grained material in the shear zone deforming by grain size sensitive mechanisms that are weaker than the surrounding rock and the orientation that maximizes shear stress along this weak zone.
2. A preexisting fault in a strong orientation (60°) to the compression direction will not be reactivated as a ductile shear zone despite having a zone of fine-grained material

that is nominally weaker than the surrounding coarse-grained host rock. The lower shear stress due to the orientation is the likely cause for the lack of localization in these faults. However, new shear zones may form along another suitably oriented plane of weakness, such as foliation plane.

Acknowledgements

Thank you to Dr. Caleb Holyoke, who worked alongside me and assisted me throughout the experimentation and writing process. Thank you to Dr. John Peck and Dr. Molly Witter who provided edits and feedback on the report. Finally, thank you to Jake Waller, Jacob Tallon, and Maria Razo who helped me in learning how to work with equipment in the laboratory.

References Cited

Bürgmann, R., and Dresen, G. (2008). Rheology of the lower crust and upper mantle: Evidence from rock mechanics, geodesy, and field observations. *Annual Review of Earth and Planetary Sciences*, *36*(1), 531–567, https://doi.org/10.1146/annurev.earth.36.031207.124326.

H. J. Frost, and M. F. Ashby (1982) Deformation-mechanism Maps: The Plasticity and Creep of Metals and Ceramics, Elsevier Science Limited, 1982, 166 pages.

Guermani, A., and Pennacchioni, G. (1998). Brittle precursors of plastic deformation in a granite: An example from the Mont Blanc Massif (Helvetic, Western Alps). *Journal of Structural Geology*, *20*(2-3), 135–148. https://doi.org/10.1016/s0191-8141(97)00080-1

Holyoke, C. W., and Tullis, J. (2006). Mechanisms of weak phase interconnection and the effects of phase strength contrast on fabric development. *Journal of Structural Geology*, *28*(4), 621–640. https://doi.org/10.1016/j.jsg.2006.01.008

Holyoke, C. W. and Kronenberg, A. K. (2010). Accurate differential stress measurement using the molten salt cell and solid salt assemblies in the Griggs apparatus with applications to strength, piezometers and rheology, Tectonophysics, 494(1–2) 17-31, https://doi.org/10.1016/j.tecto.2010.08.001.

Kullberg, J. (2021). *Effect of Pre-Existing Heterogeneities on Strain Localization in a Foliated Granitic Gneiss*. The University of Akron, Master's Thesis, http://rave.ohiolink.edu/etdc/view?acc_num=akron1621600334762676

Mancktelow, N. S., and Pennacchioni, G. (2005). The control of precursor brittle fracture and fluid–rock interaction on the development of single and paired ductile shear zones. *Journal of Structural Geology*, *27*(4), 645–661. https://doi.org/10.1016/j.jsg.2004.12.001

Sibson, R. H. (1985). A note on fault reactivation. *Journal of Structural Geology*, *7*(6), 751–754. https://doi.org/10.1016/0191-8141(85)90150-6

Tullis, J., Dell'Angelo, L., and Yund, R.A. (1990). Ductile shear zones from brittle precursors in feldspathic rocks: The role of dynamic recrystallization, in Duba, A.G., Durham, W.B., Handin, J.W., and Wang, H.F. eds., Geophysical Monograph Series, Washington, D. C., American Geophysical Union, v. 56, p. 67–81, https://doi.org/10.1029/GM056p0067h.

Tullis, J., and Yund, R.A., (1991). Diffusion creep in feldspar aggregates: experimental evidence: Journal of Structural Geology, v. 13, p. 987–1000, https://doi.org/10.1016/0191-8141(91)90051-Jh

Zurbriggen, R., Kamber, B.S., Handy, M.R., and Nägler, T.F., 1998, Dating synmagmatic folds: a case study of Schlingen structures in the Strona-Ceneri Zone (Southern Alps, northern Italy): DATING SYNMAGMATIC FOLDS: Journal of Metamorphic Geology, v. 16, p. 403–414, https://doi.org/10.1111/j.1525-1314.1998.00145.x.

Tables and Figures

Table 1 - List of experiments. All experiments performed at T = 750°C, P_c = 1.5 GPa and strain rate of ~ $6.8*10^{-7}$/s and foliation in all cores oriented at 45° to the compression direction.

Experiment	Artificial fault orientation	Total strain (%)	Peak stress[1] (MPa)	Final stress[2] (MPa)	Time at conditions (hr)
Z-227	45°	8	600	-	89
Z-239	45°	40	740 (9%)	380	183
Z-238	60°	34	670 (14%)	560	191

[1] - strain at peak stress in parentheses if different than final strain

[2] - if different from peak stress

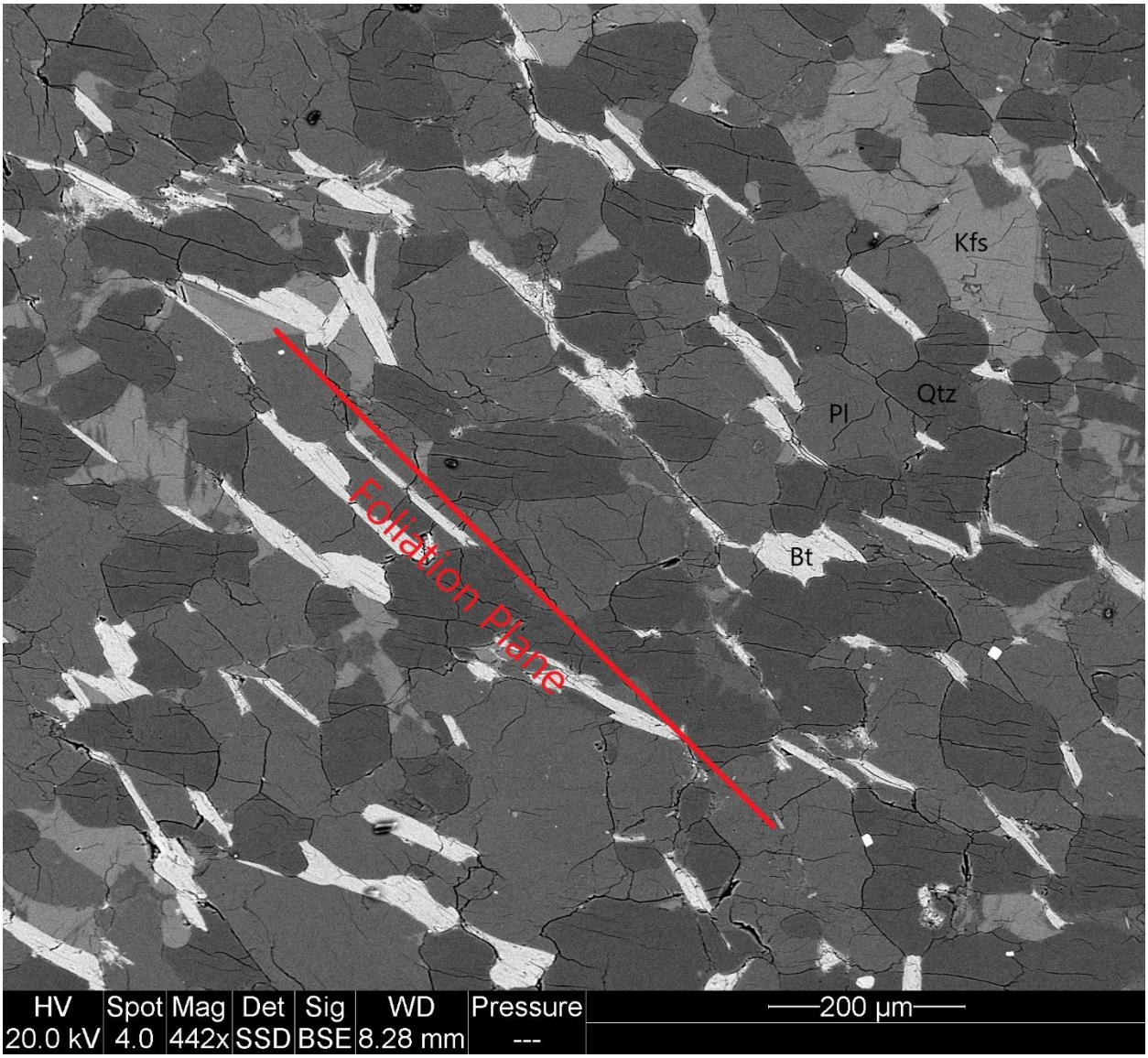

Figure 1. SEM-BSE images of undeformed Gneiss Minuti starting material. The foliation defined by parallel biotite grains is oriented at ~45° to the edges of the image. Biotite, potassium feldspar, plagioclase and quartz grains are successively darker shades of gray.

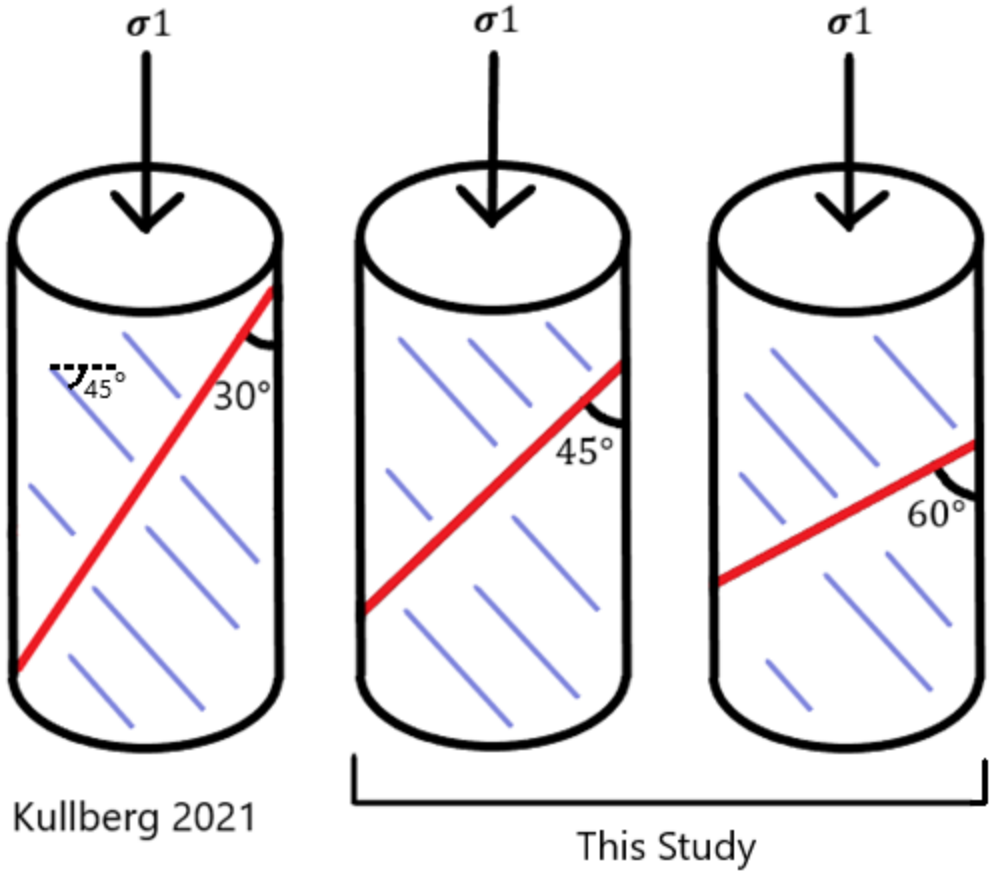

Figure 2: The foliation (blue lines) in all cores was oriented at 45° to the compression direction. Kullberg (2021) deformed cores with a pre-fault (red line) at ~30° to the compression direction, crosscutting the foliation (left-most cylinder above). The orientations of the artificial faults (red lines) in experiments in this study were at 45° and 60° to the compression direction, crosscutting the foliation (center and right-most cylinder above).

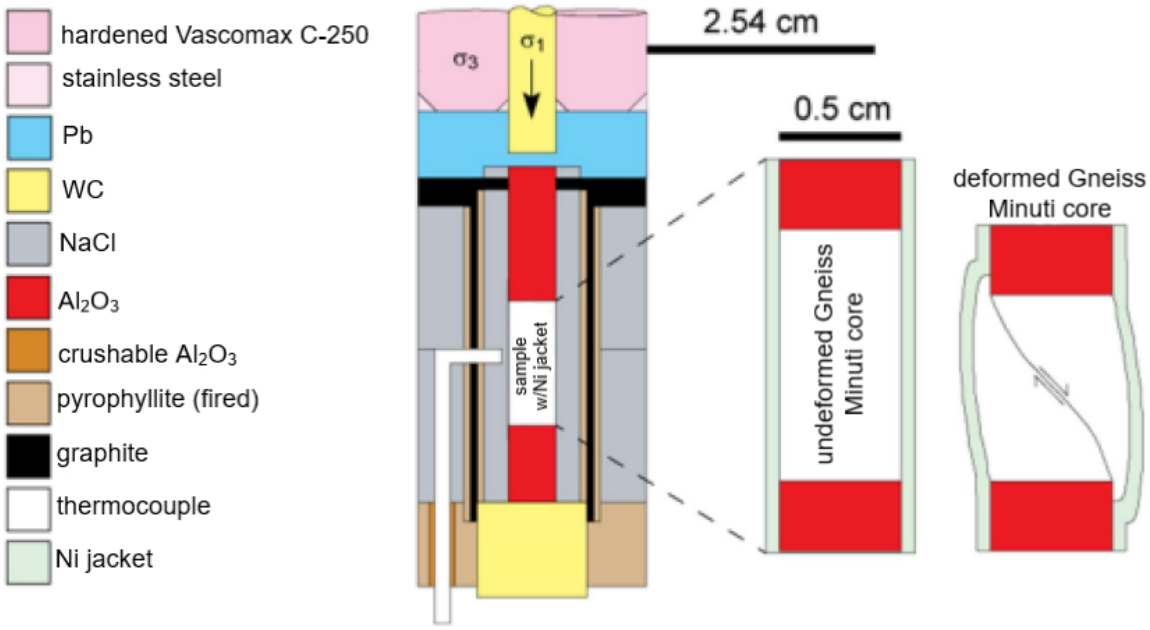

Figure 3: Experiments were performed in a Griggs-type deformation apparatus using a solid salt assembly.

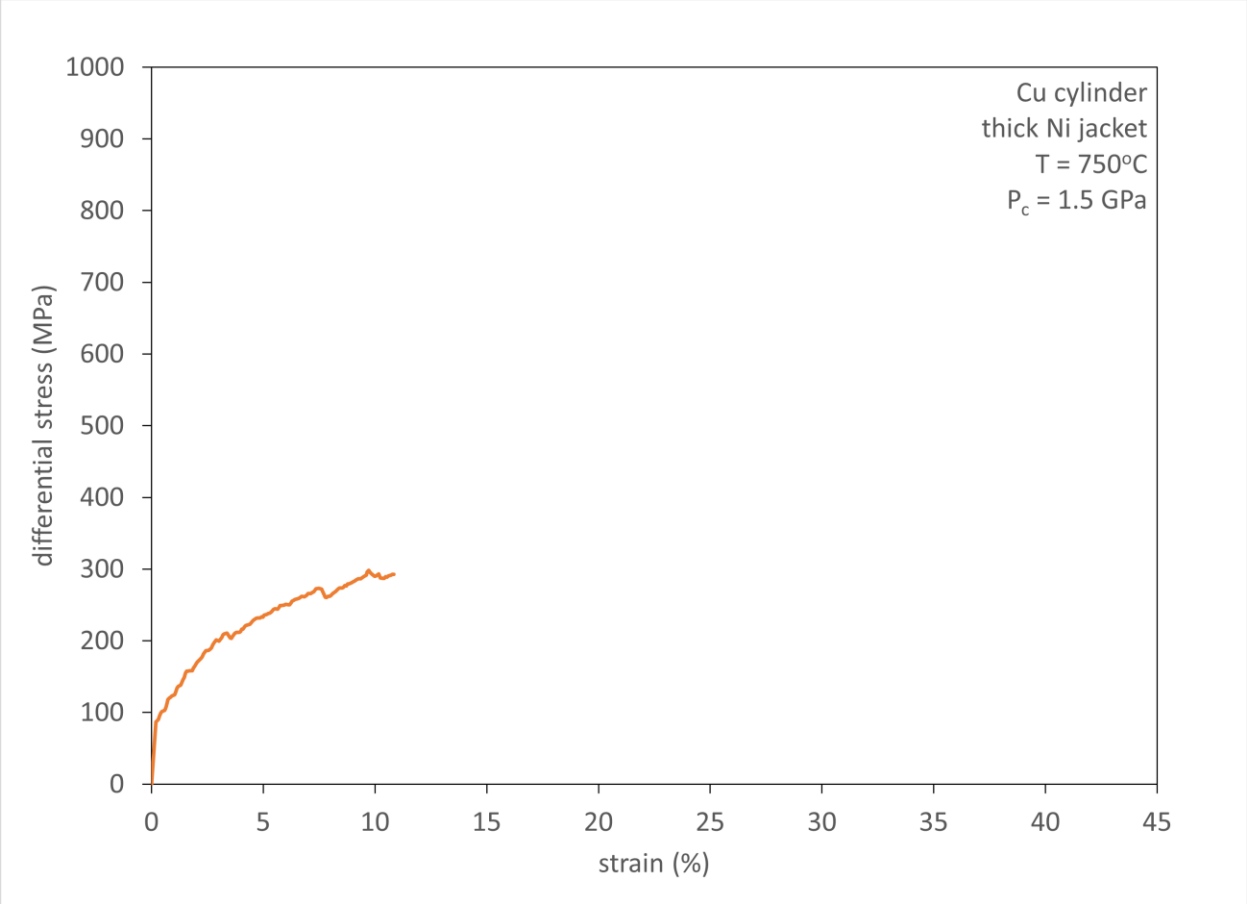

Figure 4: The strength of a Cu cylinder in a thick Ni jacket was measured to correct the strength of Gneiss Minuti cores for the strong thick Ni jacket used in those experiments.

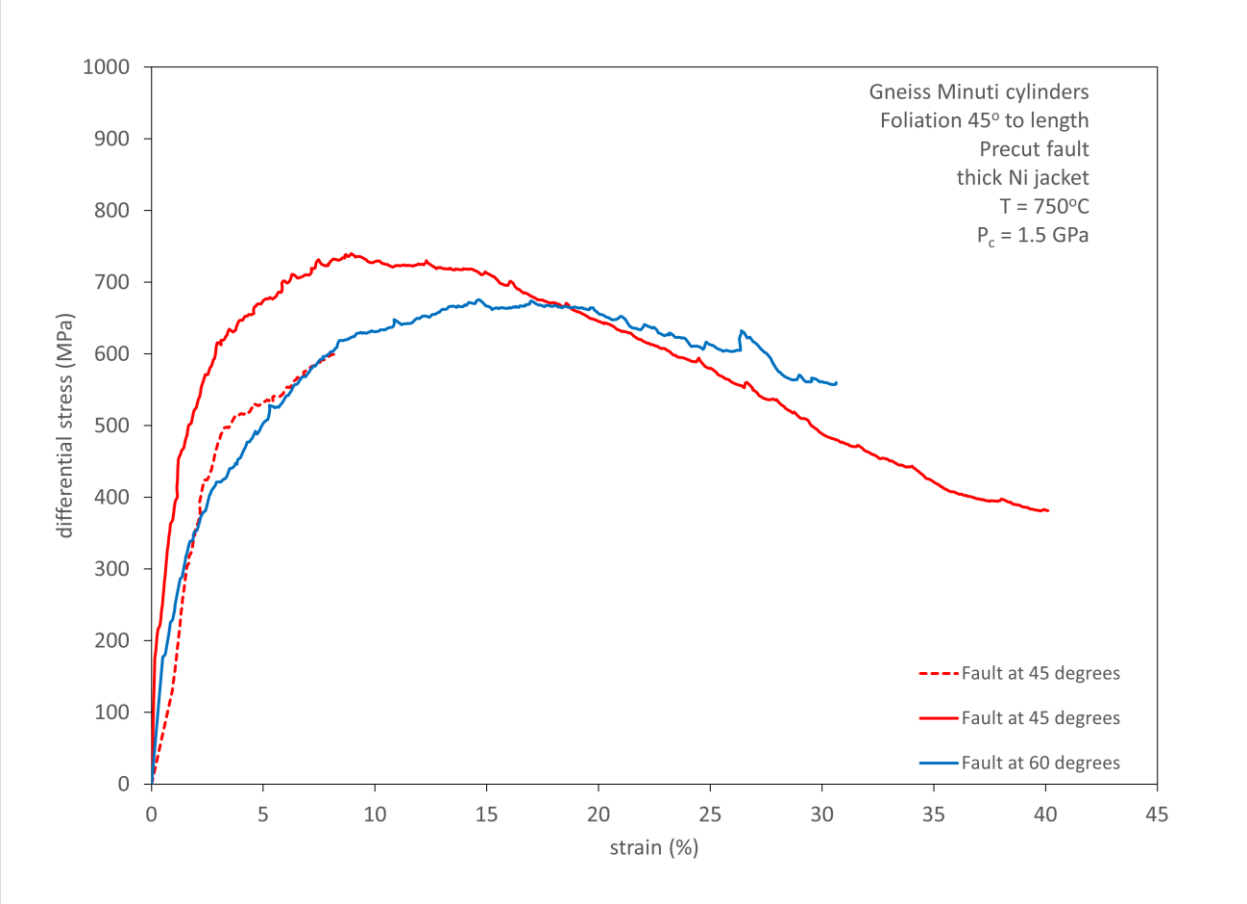

Figure 5: Peak strengths of Gneiss Minuti cylinders with artificial faults of different orientations are similar. However, the core with an artificial fault oriented at 45° to the compression direction deformed to high strain (solid red line) strain-weakened considerably more than the core with the artificial fault oriented at 60° to the compression direction (solid blue line).

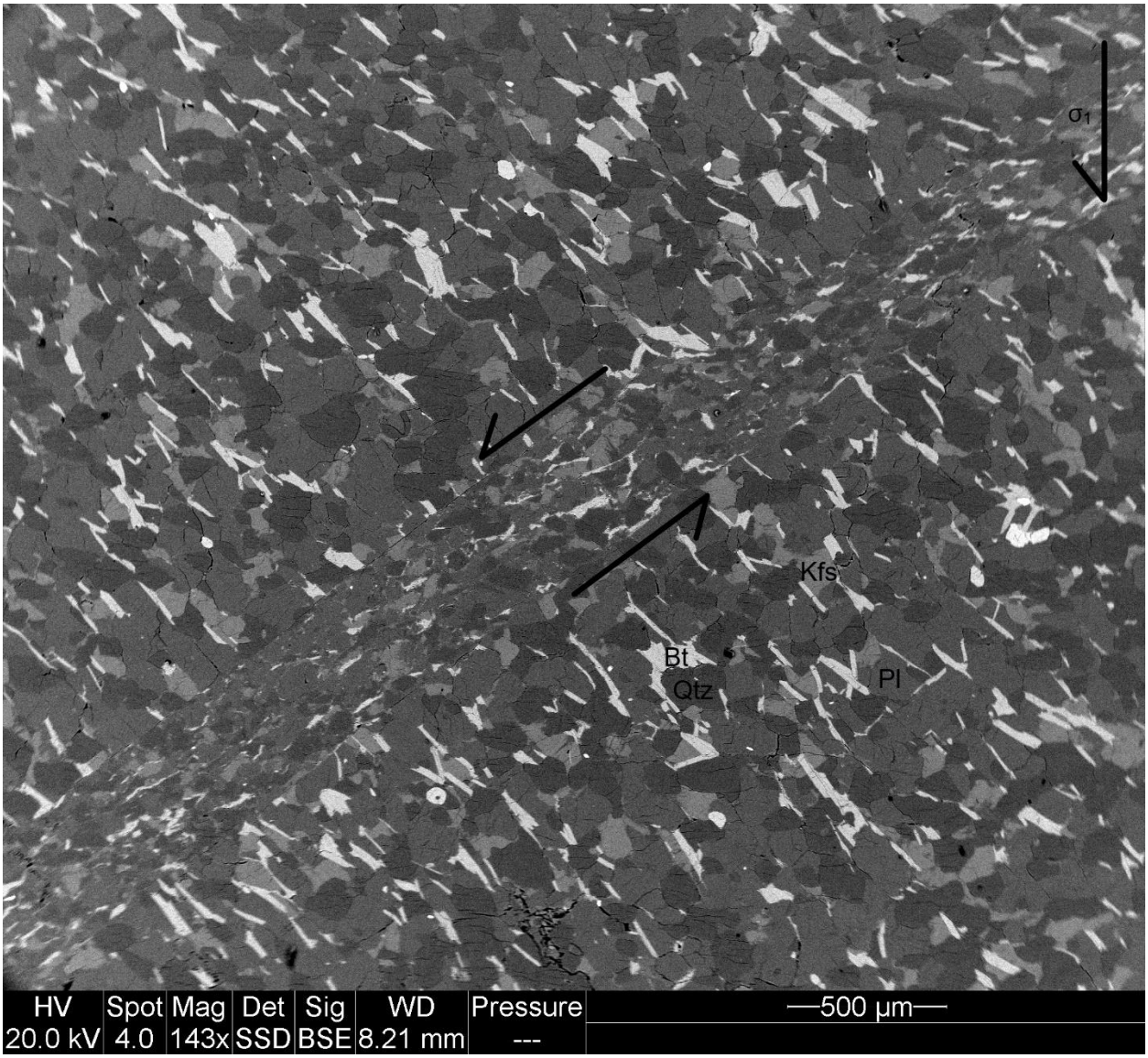

Figure 6: SEM-BSE image of Gneiss Minuti with an artificial fault oriented at 45° to the compression direction, deformed to low strain (ε = 8%). The host rock is undeformed and strain appears to be localized within the artificial fault.

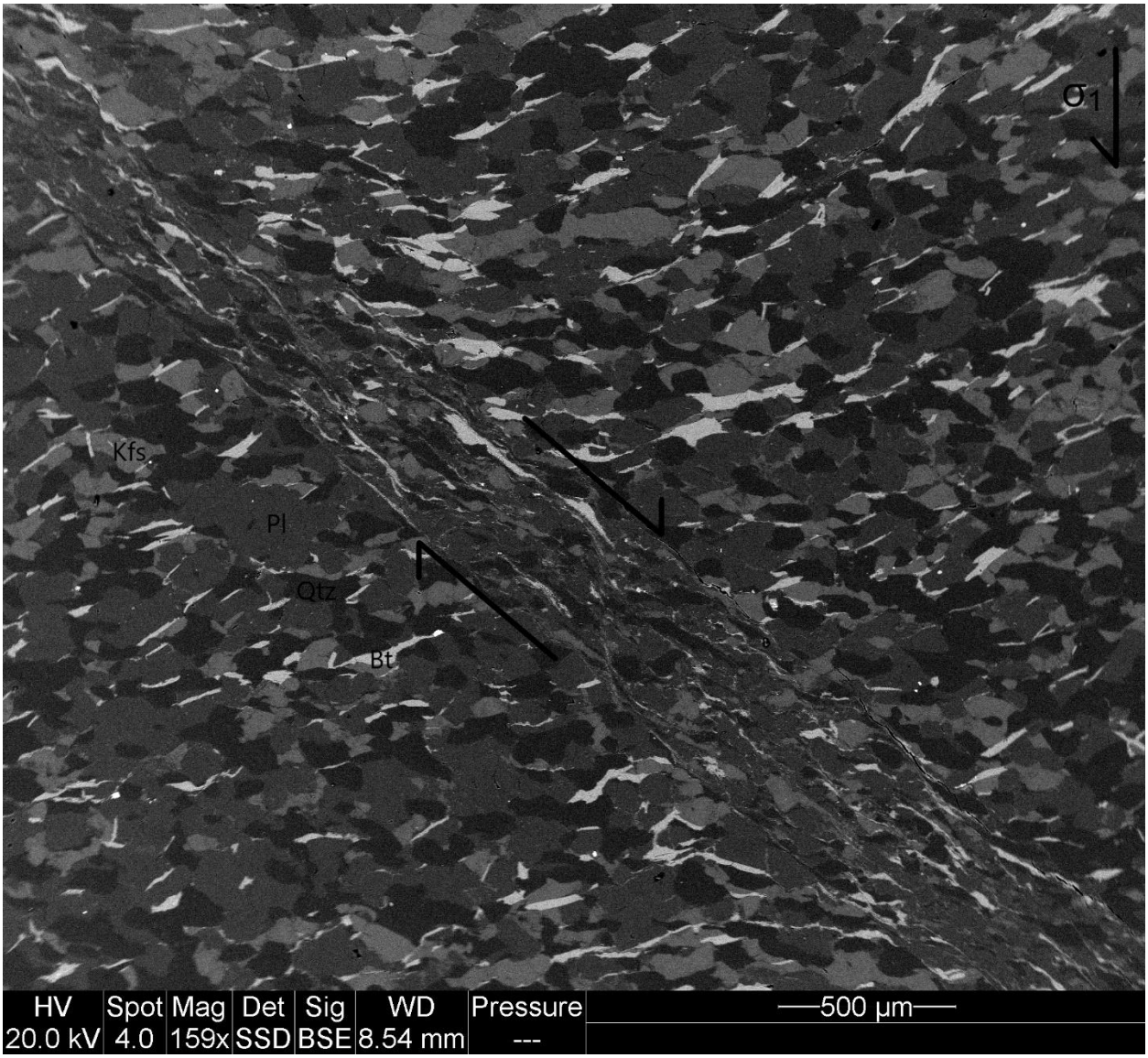

Figure 7: SEM-BSE image of Gneiss Minuti with an artificial fault oriented at 45° to the compression direction. Strain is primarily localized along the artificial fault, but the foliation is also rotated near the artificial fault indicating that some strain was accommodated by the host rock.

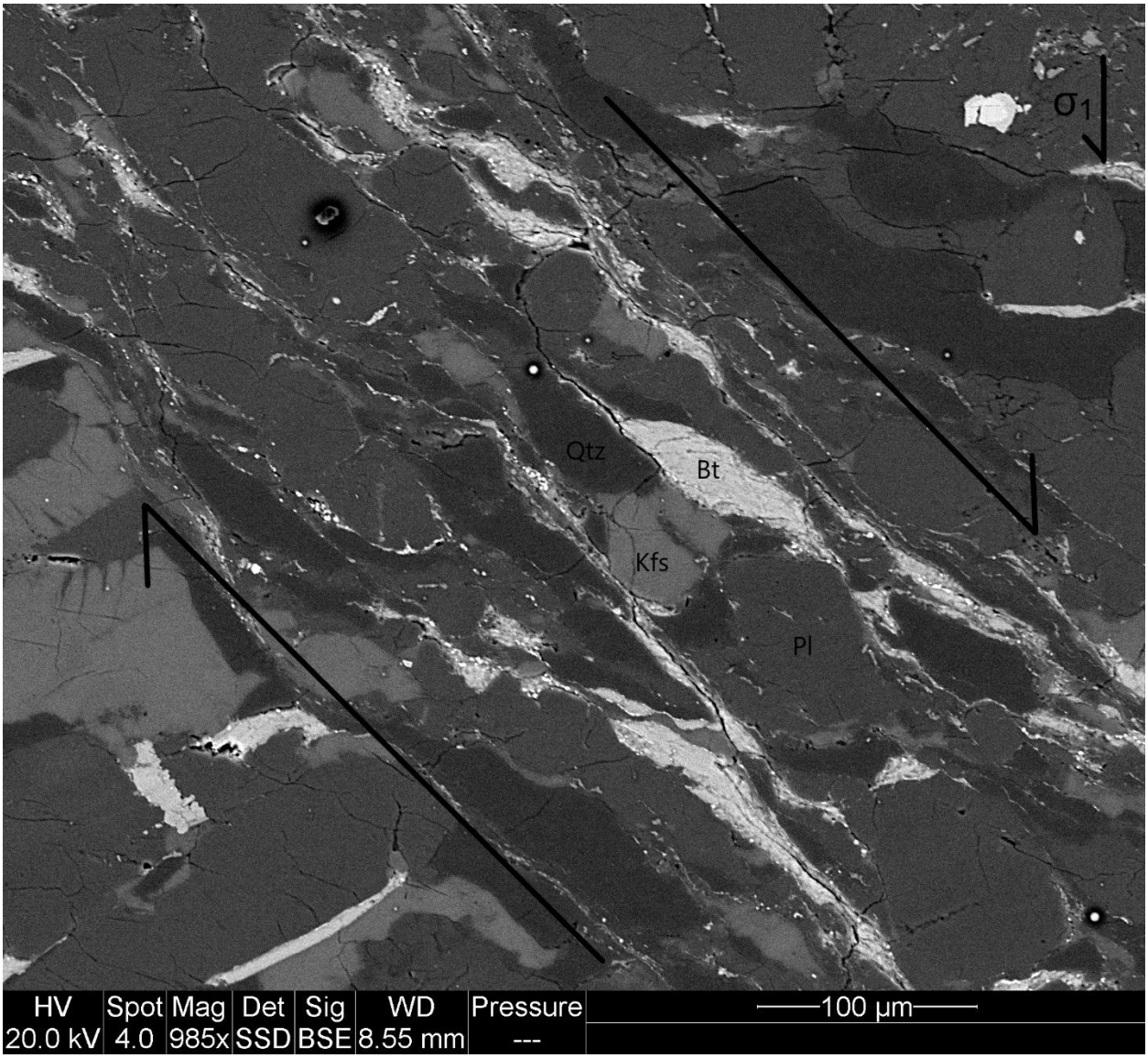

Figure 8: Grains within the shear zone are highly sheared (SEM-BSE image). Biotite grains form mica fish, with long tails of fine-grained biotite parallel to the shear zone.

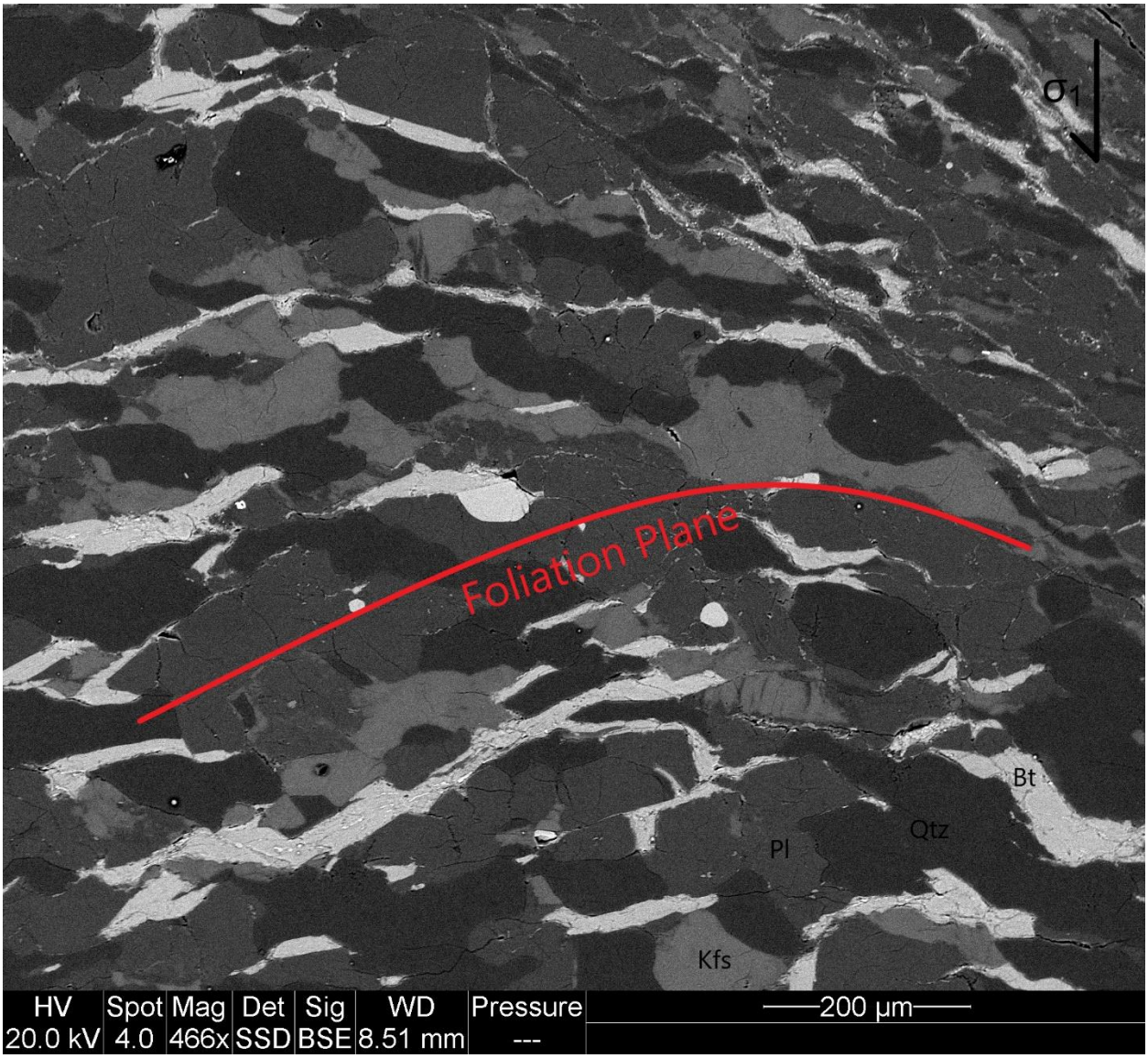

Figure 9: Foliation in the host rock near the shear zone curves towards the artificial fault indicating some deformation of the host rock (SEM-BSE image).

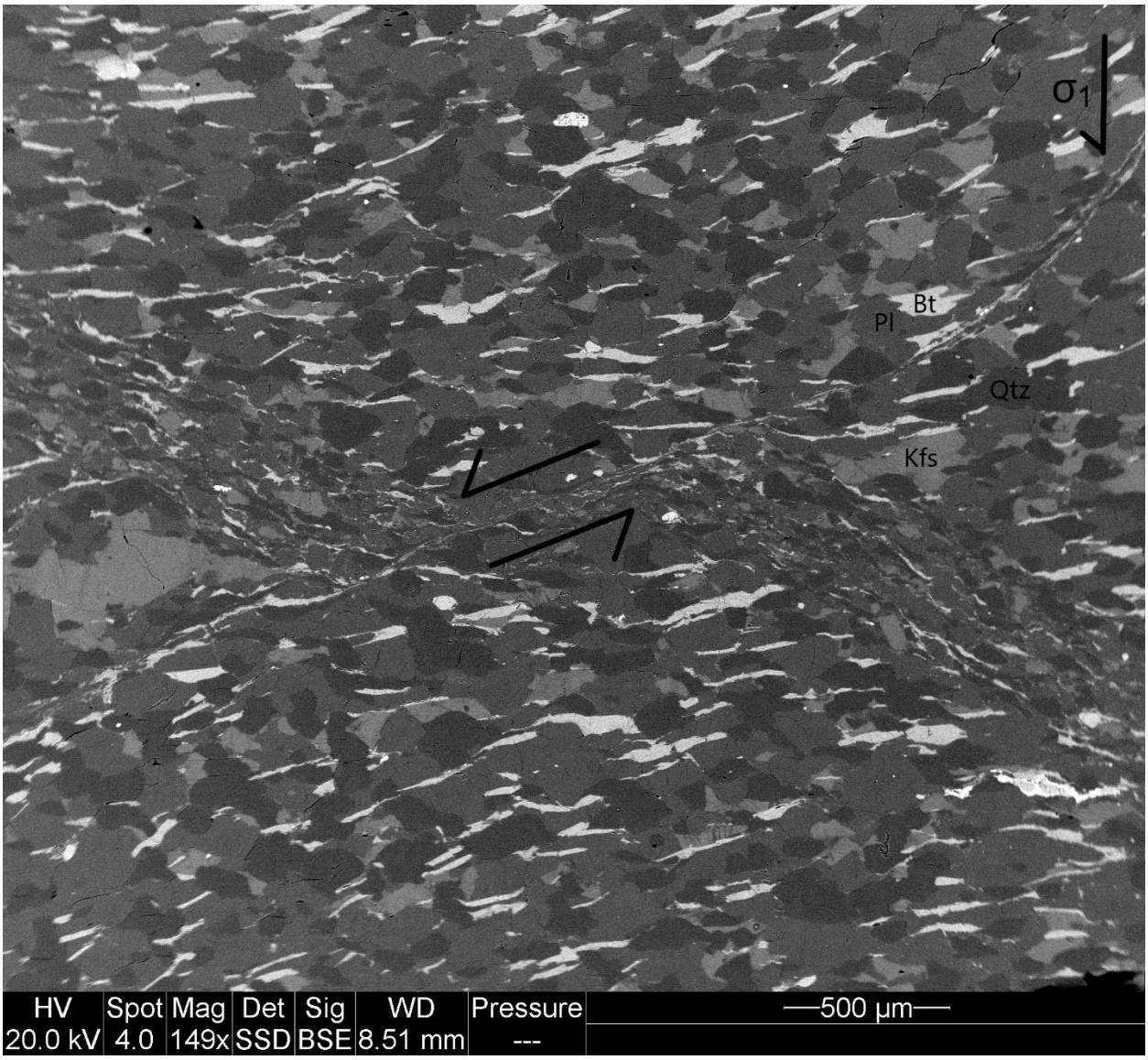

Figure 10: SEM-BSE image of Gneiss Minuti with an artificial fault oriented at 60° to the compression direction. The artificial fault is offset by a new shear zone which cross cuts the foliation. The foliation in the host rock is also significantly rotated, indicating that strain is primarily accommodated outside of the artificial fault.

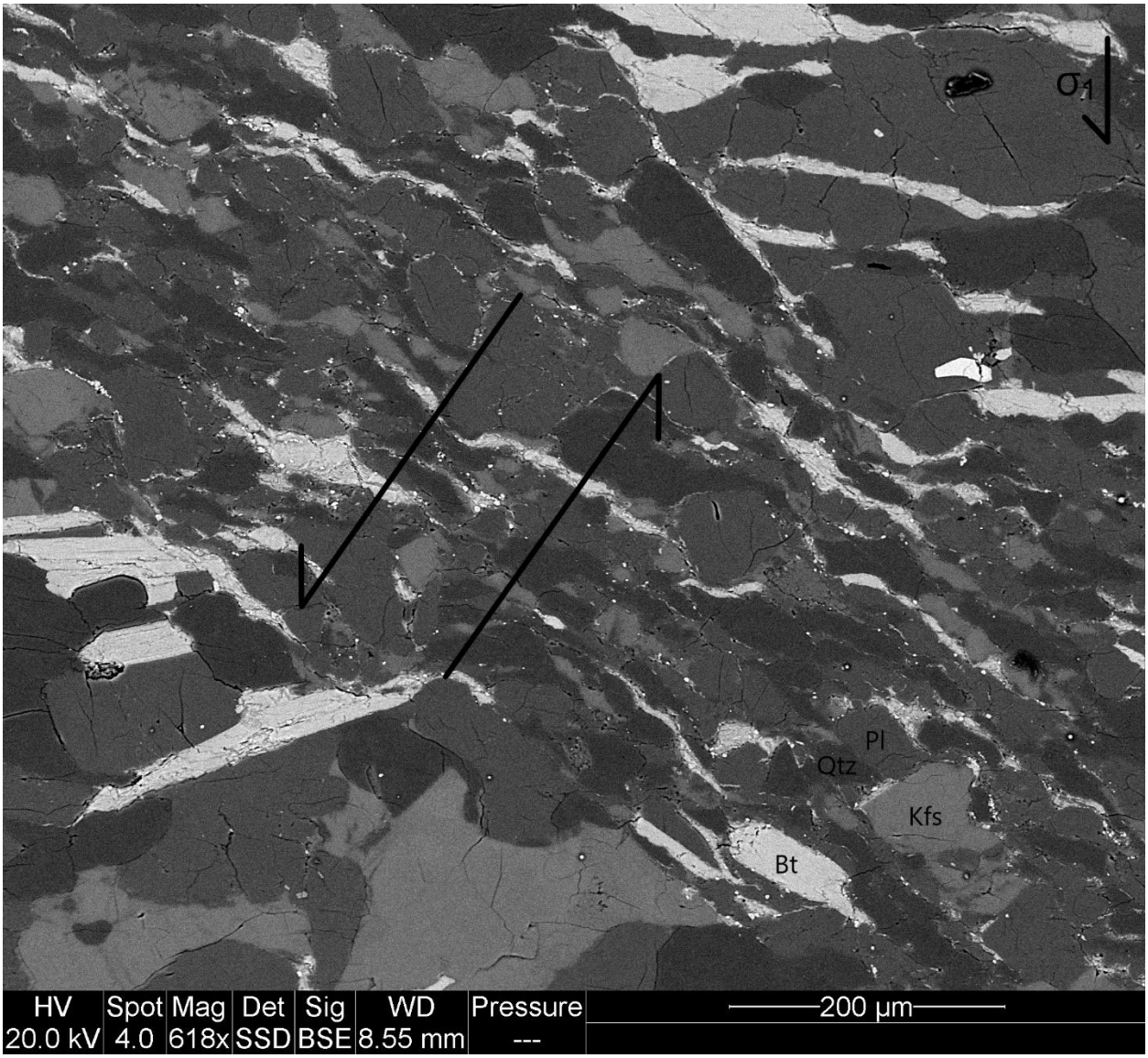

Figure 11: Micro-faults parallel to the foliation cross-cut grains within the artificial fault (SEM-BSE image). Grains within the artificial fault are flattened, but do not have significant tails of recrystallized grains.

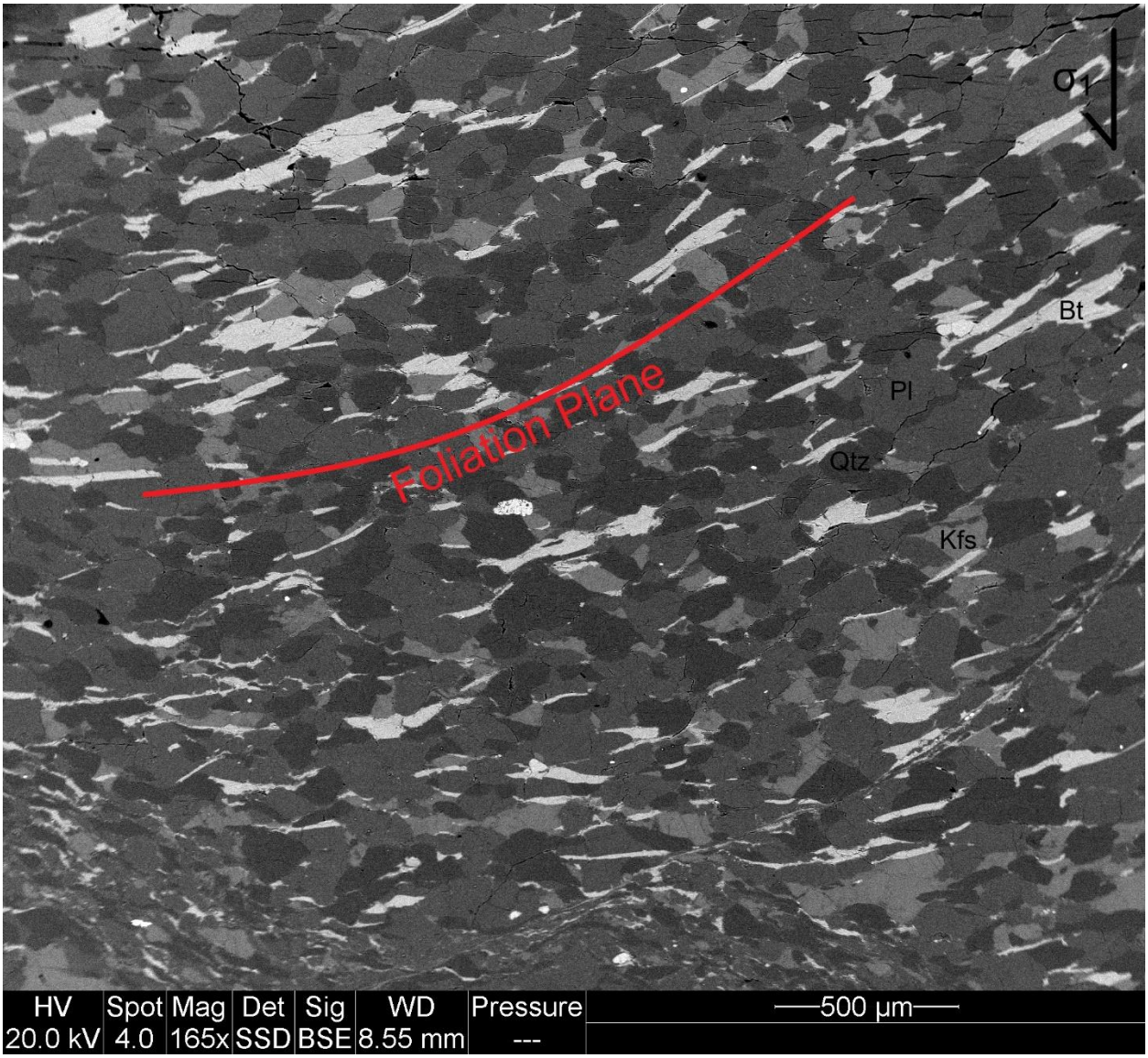

Figure 12: Foliation outside of the artificial fault is curved towards the shear zone and a small-scale shear zone cross cuts the artificial fault, indicating that strain is accommodated primarily outside of the artificial fault (SEM-BSE image).

Appendix 1

Experiments not used in main study

Two experiments were performed at the same conditions as the other experiments described in the main body of text, but with weak Ag jackets instead of strong Ni jackets. The samples were significantly during pressurization, which makes the starting condition unknown and therefore, these experiments were not useful for this study.

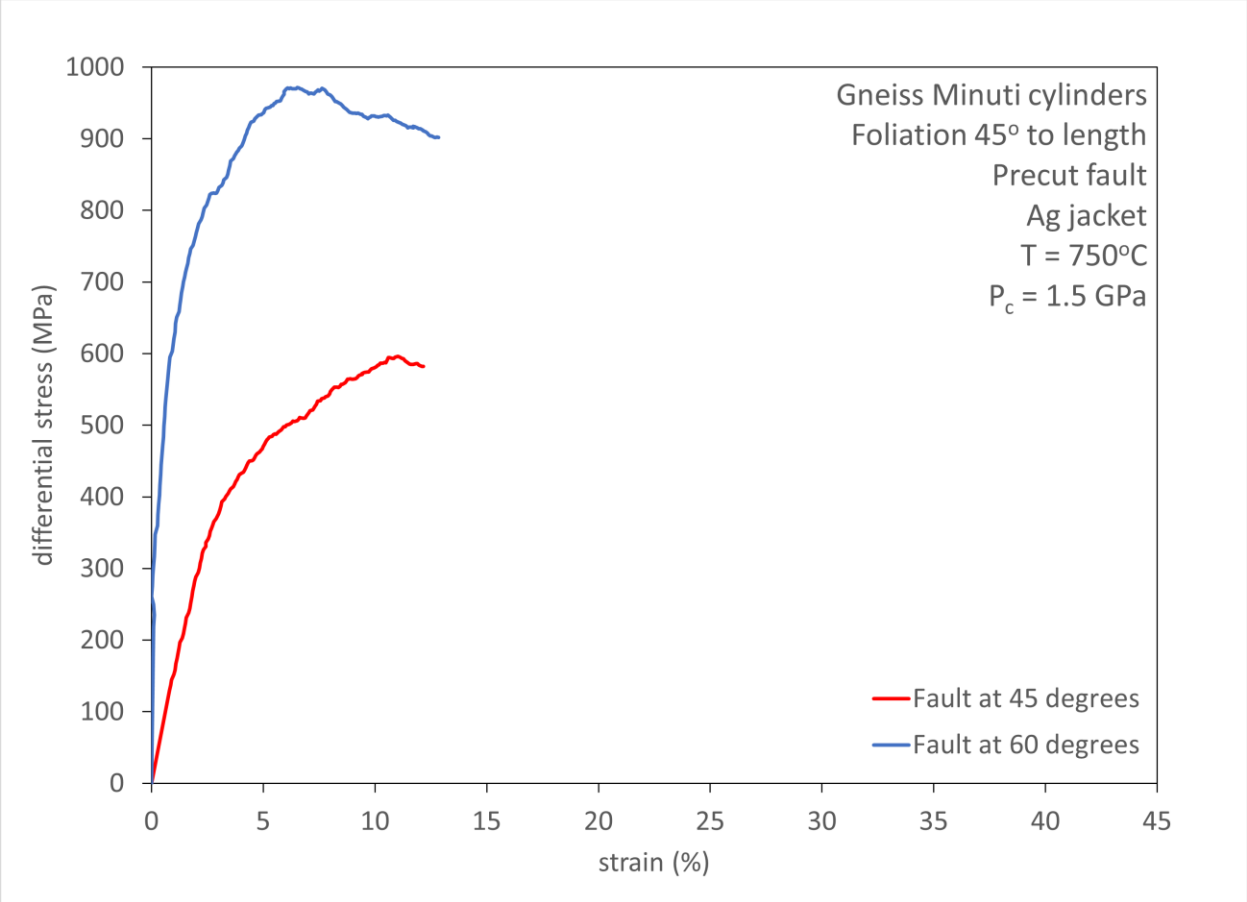

Figure A1: Mechanical data from two experiments performed on Gneiss Minuti cores using an Ag jacket (SEM-BSE image).

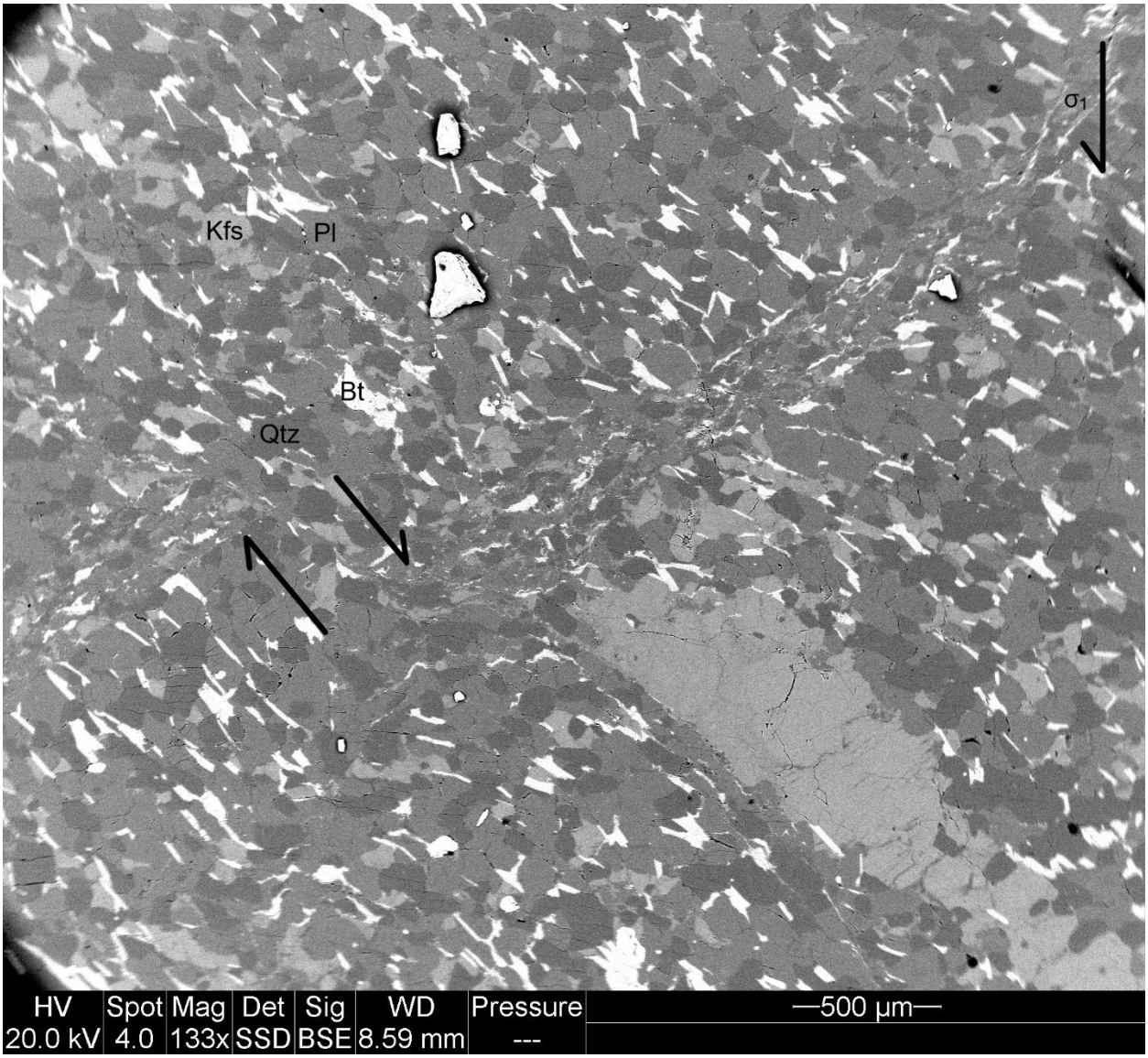

Figure A2: The Ag jacketed experiment with an artificial fault at 45° Showed one large offset of the artificial fault caused by a new shear zone forming along the foliation plane (SEM-BSE image).

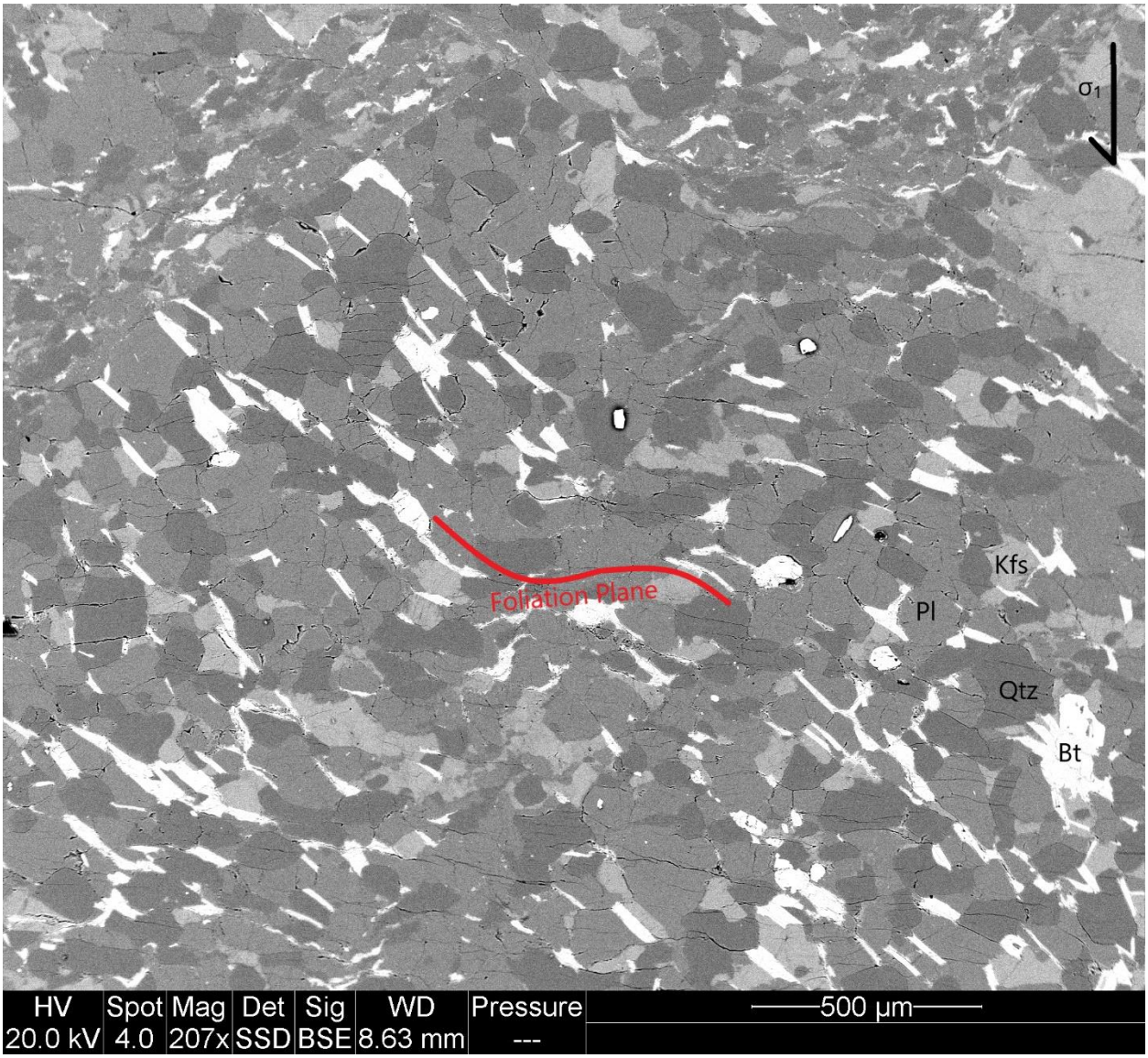

Figure A3: Foliation curved into an orientation aligned with the artificial fault (SEM-BSE).

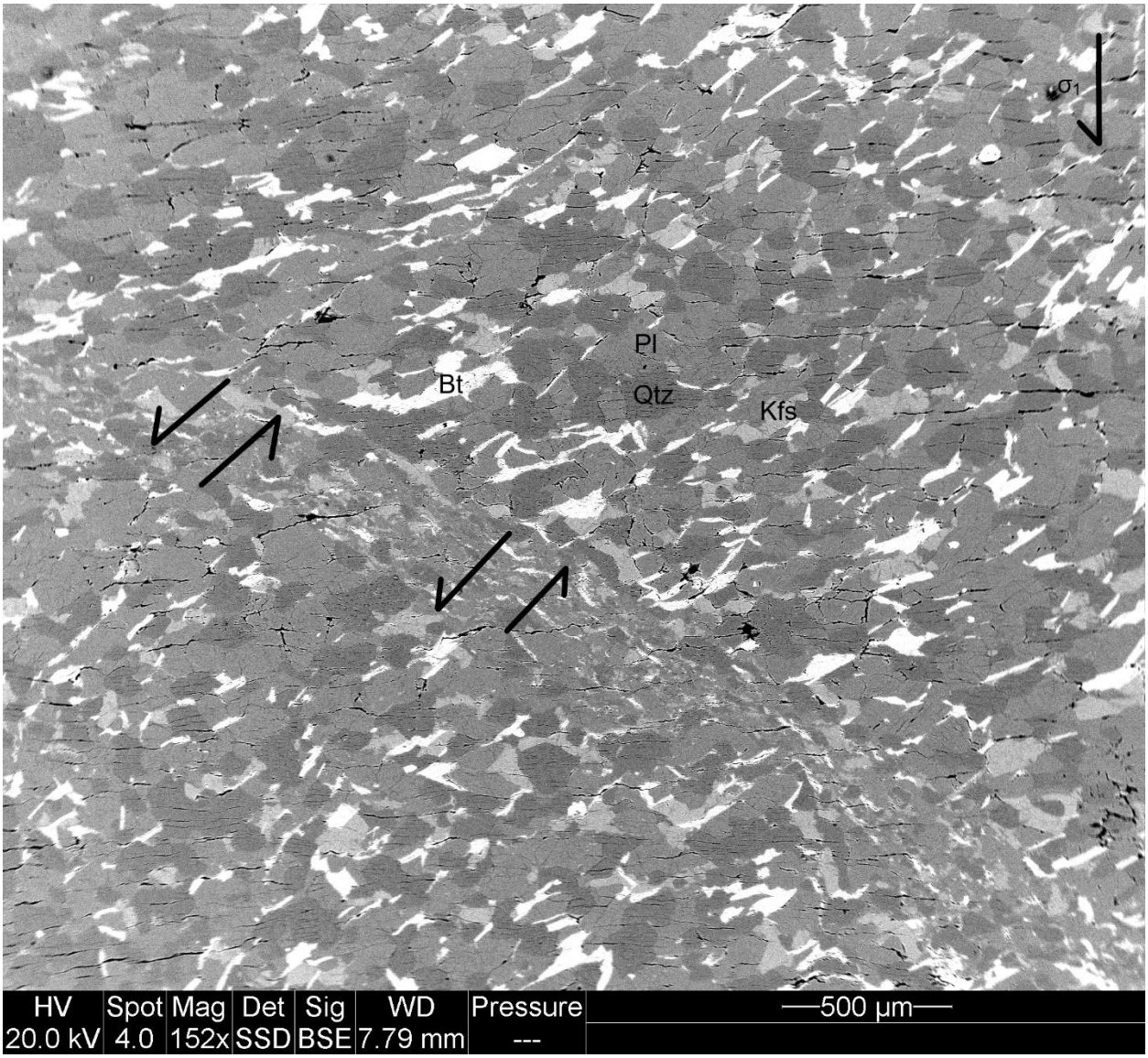

Figure A4: The Ag jacketed experiment with an artificial fault at 60^{o} had significant offset of the artificial fault in multiple locations aligned with the foliation plane. The foliation was also curved outside the artificial fault (SEM-BSE image).

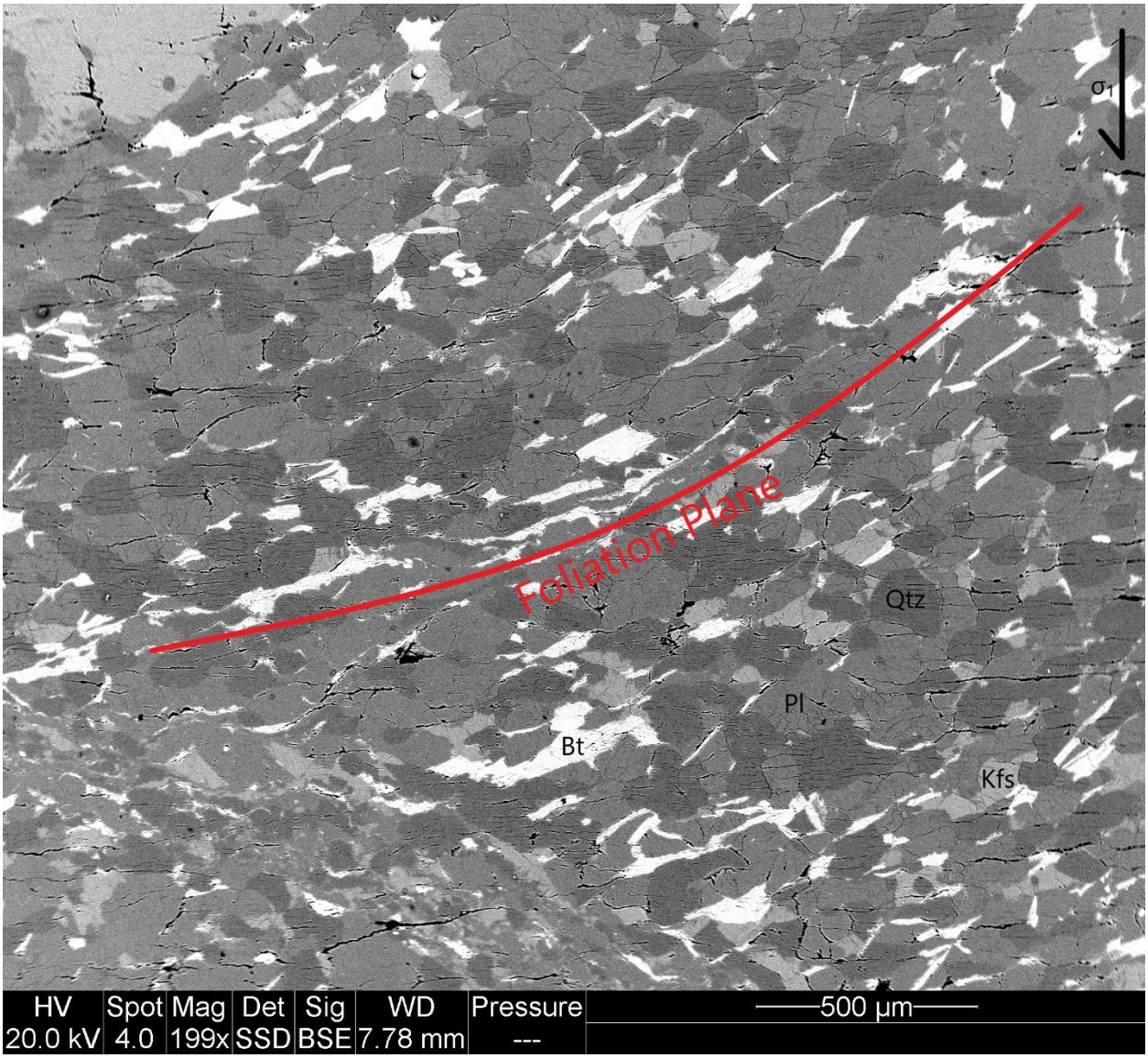

Figure A5: Foliation curves outside the artificial fault, indicating that strain is accommodated mostly outside of the artificial fault (SEM-BSE image).